



Universiteit
Leiden
The Netherlands

The effect of lipid composition on the thermal stability of nanodiscs

Knetsch, T.G.J.; Ubbink, M.

Citation

Knetsch, T. G. J., & Ubbink, M. (2023). The effect of lipid composition on the thermal stability of nanodiscs. *Biochimica Et Biophysica Acta - Biomembranes*, 1866(1).
doi:10.1016/j.bbamem.2023.184239

Version: Publisher's Version

License: [Creative Commons CC BY 4.0 license](#)

Downloaded from: <https://hdl.handle.net/1887/3728253>

Note: To cite this publication please use the final published version (if applicable).



The effect of lipid composition on the thermal stability of nanodiscs

Tim G.J. Knetsch, Marcellus Ubbink*

Leiden Institute of Chemistry, Leiden University, Einsteinweg 55, 2333 CC Leiden, the Netherlands

ARTICLE INFO

Keywords:
Nanodiscs
Lipid composition
Thermal stability
Multi-angle light scattering

ABSTRACT

Discoidal lipid nanoparticles (LNPs) called Nanodiscs (NDs) are derived from human high-density lipoprotein (HDL). Such biomimetics are ideally suited for the stabilization and delivery of pharmaceuticals, including chemicals, bio-active proteins and vaccines. The stability and circulation lifetimes of reconstituted HDL nanoparticles, including NDs, are variable. Lipids found in thermophilic archaea and bacteria are prime candidates for the stabilization of LNPs. We report the thermal stability of NDs prepared with lipids that differ in saturation, have either ether- or ester linkages between the fatty acid and glycerol backbone or contain isoprenoid fatty acid tails (phytanyl lipids). NDs with two saturated fatty acids show a much greater long-term thermostability than NDs with an unsaturated fatty acid. Ether fatty acid linkages, commonly found in thermophiles, did not improve stability of NDs compared to ester fatty acid linkages when using saturated lipids. NDs containing phytanyl and saturated alkyl fatty acids show similar stability at 37 °C. NDs assembled with phytanyl lipids contain three copies of the membrane scaffolding protein as opposed to the canonical dimer found in conventional NDs. The findings present a strong basis for the production of thermostable NDs through the selection of appropriate lipids and are likely broadly applicable to LNP development.

1. Introduction

Protein-lipid nanodiscs (NDs) are nanometer size discoidal particles of lipid membrane stabilized by a protein dimer that wraps around the hydrophobic alkyl chains like a belt. The initial NDs were developed and popularized by Steven G. Sligar and co-workers [1,2]. These NDs are prepared using membrane scaffolding proteins (MSPs), derived from Apolipoprotein A1 (ApoA1); the most abundant protein in high-density lipoprotein (HDL). In the human body, HDL is involved in the process of reverse cholesterol transport and is often referred to as “good cholesterol” [3]. NDs are mostly used for the reconstitution of membrane proteins into a near-native lipid environment of controlled size and composition for biochemical and structural studies. Various types of reconstituted HDL (rHDL), including NDs, have also shown great potential as drug or vaccine delivery systems and have been extensively reviewed as such [4–7]. These biomimetic lipid nanoparticles (LNPs) have inherently good biocompatibility and biodegradability, because rHDL is adapted from an endogenous molecular transport system [4]. Indeed, CSL112, a formulation of discoidal rHDL, was well tolerated by patients at very high doses of four weekly infusions of 6 g and has reached phase 3 clinical trials [8,9]. Recombinant ND-based vaccines have shown promising results in mice and non-human primates in the

treatment of cancer [10–12]. For many viruses, such as influenza, human immunodeficiency virus (HIV) and severe acute respiratory syndrome coronavirus (SARS-CoV – 2), the surface glycoproteins are responsible for viral attachment and entry. Viral spike proteins are recognized as the primary antigen by the immune system and are prominent vaccine targets [13–16]. It was reported that mice immunized with NDs containing the influenza hemagglutinin (HA) spike protein had significantly higher anti-HA IgG titer than mice immunized with HA alone and the HA-ND elicited a more broadly neutralizing antibody response. Intranasal and intramuscular administration of HA-NDs were equally effective at eliciting an immune response as a commercially available vaccine [17].

Unfortunately, preparations of rHDL have shown large variation in biodistribution and circulation half-life [5]. NDs can be stored at 4 °C up to months without significant aggregation [18,19]. However, incubation at physiological temperature results in irreversible breakdown and aggregation of NDs over the course of a few hours to days. The necessity for cold-chain distribution of biopharmaceuticals significantly complicates mass vaccination efforts against seasonal pathogens, especially in areas where refrigeration is scarce. Thus, thermostable NDs are highly desirable for the pharmaceutical industry. Additionally, thermostable ND vaccines could lengthen the antigen circulation lifetime and

* Corresponding author.

E-mail address: m.ubbink@chem.leidenuniv.nl (M. Ubbink).

<https://doi.org/10.1016/j.bbamem.2023.184239>

Received 11 August 2023; Received in revised form 6 October 2023; Accepted 16 October 2023

Available online 20 October 2023

0005-2736/© 2023 The Authors. Published by Elsevier B.V. This is an open access article under the CC BY license (<http://creativecommons.org/licenses/by/4.0/>).

subsequently increase immunogenicity of the formulation. Low stability at ambient temperature significantly limits the use of NDs as a stable carrier system and has led to optimization of NDs towards higher stability. For example, MSPs have been covalently linked between the N- and C-termini to produce covalently circularised NDs (cNDs), showing improved stability and homogeneity [20–23]. In addition, ND stability and solubility have been improved by the introduction of additional negative charges on the scaffold protein or lipid head groups, increasing inter-particle repulsion and consequently reducing aggregation propensity [24,25].

Thermostability of discoidal rHDL was shown to be correlated to the acyl chain length of the incorporated lipids. rHDL composed of lipids with increasing acyl chain lengths exhibit increasing thermostability [26]. Furthermore, cis-unsaturation was shown to have a destabilizing effect, as faster unfolding of ApoC1 was observed by circular dichroism (CD) spectroscopy for rHDL comprising mono- or polyunsaturated lipids compared to saturated lipids [26]. The stabilizing effects of fatty acid saturation and increasing lipid acyl chain length on rHDL were attributed to the more extensive intramolecular lipid-lipid and protein-lipid interactions. Lipoprotein remodeling refers to the processes that regulate the composition, structure, and functionality of lipoprotein particles. HDL remodeling is facilitated by enzymes such as lecithin cholesterol acyltransferase (LCAT), cholesteryl ester transfer protein (CETP) and phospholipid transfer protein (PLTP). The ability of endogenous enzymes such as LCAT to interact with and subsequently remodel rHDL depends on both the protein and lipid composition [27–30]. In the presence of bovine serum and rat plasma, rHDL comprising saturated lipids with long acyl chains proved to be more stable than their shorter and unsaturated counterparts [30,31].

Another strategy to improve rHDL and ND stability would be through the incorporation of specialized thermostable lipids derived from thermophilic archaea or bacteria. Liposomes prepared using archaeal lipids (archaeosomes) have shown increased tolerance to phospholipase activity, oxidative stress, detergents, heat and acidity [32]. Archaeal lipids are chemically different from bacterial and eukaryotic phospholipids. Their acyl chains are almost exclusively saturated and contain isoprenoid fatty acids that are *sn*-2, 3 linked to the glycerol backbone through ether bonds, whereas in bacteria and eukarya fatty acids are *sn*-1, 2 linked, primarily by ester bonds. Ether-linked phospholipids cannot be processed by LCAT, which could enhance the circulation life time of an *in vivo* drug delivery system based on these lipids [27]. Incorporation of such lipids could simultaneously improve ND stability and act as vaccine adjuvants, molecules that can potentiate the immune response [33–36]. The co-delivery of antigen/adjuvanting lipid NDs to dendritic cells in lymph nodes was reported to enhance the immune response to recombinant antigens [37,38]. Traditionally, archaeosomes are prepared using total polar lipid extracts, which makes it impossible to accurately determine the effect of individual lipids on stability of the nanoparticle. Data from Batavia Biosciences B.V. describe the preparation of thermostable NDs using synthetic lipids that resemble those found in thermophilic archaea. These NDs show increased thermostability compared to conventional NDs prepared with 1- palmitoyl-2-oleoyl-*sn*-glycero-3-phosphocholine (POPC) lipids [39]. The use of well-defined chemically synthesized lipids is much more attractive from a safety and drug development perspective than using heterogeneous natural isolates. In this study, core lipid structural elements were systematically varied to get a clear understanding of the structure-stability relationships of NDs assembled with different phospholipids. The degree of saturation and the presence of ether - or ester linkages between the fatty acid and glycerol backbone were compared. The effect of isoprenoid fatty acids (phytanyl moieties), mainly found in archaeal lipids, was also examined. The lipids studied in this work comprise the ester PC lipids POPC, 1,2-dipalmitoyl-*sn*-glycero-3-phosphocholine (DPPC), their respective ether analogs 1-O-hexadecanyl-2-O-(9Z-octadecenyl)-*sn*-glycero-3-phosphocholine (16o18oPC) and 1,2-di-O-hexadecyl-*sn*-glycero-3-phosphocholine (D16oPC) and the phytanyl ester lipid 1,2-

diphytanoyl-*sn*-glycero-3-phosphocholine (DPhPC) and ether analog 1,2-di-O-phytanyl-*sn*-glycero-3-phosphocholine (DPhoPC). The structures are shown in Fig. 1.

2. Results

2.1. Formation and characterization of NDs using ester- and ether-linked, linear- and branched lipids

NDs were prepared by reconstitution of dried lipid into buffer containing cholate detergent together with purified MSP1D1 protein. ND formation was initiated by detergent removal through dialysis or incubation with detergent absorbing bio-beads near the respective lipid phase transition temperatures. The resulting mixtures were purified by size-exclusion chromatography (SEC), initial SEC purifications and dynamic light scattering (DLS) intensity distributions of the ND main peak fractions are shown for each type of NDs in Fig. S1 and – S2, respectively. Monodisperse NDs were produced using each of the lipids, after optimizing incubation temperatures and protein-lipid stoichiometric ratios (see Materials and Methods). Analytical SEC coupled to multi-angle light scattering (SEC-MALS) was used to establish the molecular weight of the NDs and the weight fractions of protein and lipid, from which the number of lipid molecules per ND can be derived (Table 1). Results of the biophysical characterization are illustrated for POPC NDs in Fig. 2.

Unexpectedly, it was found that not all NDs consist of the canonical double MSP belt. Although being almost identical in hydrodynamic volume and molecular weight to POPC NDs, NDs assembled with branched DPhPC- and DPhoPC lipids comprise three copies of MSP1D1 (Fig. 3). The phytanyl lipid NDs also have a comparatively small lipid weight fraction, which can be partially explained by the larger area per lipid of DPhPC and DPhoPC, compared to alkyl lipids [40,41]. An overview of the NDs weight fraction and composition is given in Table 1. To establish the amount of lipid present in DPhPC - and DPhoPC NDs independently, the total phosphorous content was also determined in a separate experiment, confirming the results from the SEC-MALS analysis (Table S1 & Fig. S3).

2.2. Thermal stability of NDs depends greatly on the lipid membrane

To compare the stability of NDs, DLS, CD spectroscopy, differential fluorimetry (nanoDSF) and analytical SEC were used. CD and nanoDSF primarily report on the unfolding of the alpha helical MSP1D1 (data not shown). Therefore, these techniques are not suitable to visualize and compare the stability and aggregation states of whole NDs. SEC-MALS provides a clear view of the aggregation states and was used in further analysis. NDs were subjected to incubation at temperatures of 20 °C, 37 °C and 50 °C for a few hours up to one day. After incubation, each sample was stored at 4 °C until SEC-MALS analysis. Resulting elution profiles were compared with the untreated control NDs kept at 4 °C throughout the experiment (Fig. 4). The study was specifically designed to test ND stability over the course of hours as opposed to a rapid temperature ramp as the former is more relevant to the transport and clinical administration of NDs. To quantify relative persistence of NDs, the elution profiles measured at A₂₈₀ were deconvoluted into separate peaks. Next, the ND peak surface area under the curve was compared with the ND surface area of the control NDs kept at 4 °C. The resulting plot of ND recovery over time is shown in Fig. 5. All types of NDs were stable at 20 °C, showing minimal to no aggregation or disintegration after 24 h. For DPPC NDs it was observed that incubations at 20 °C and 37 °C for a few hours resulted in further equilibration to a more monodisperse sample. The DPPC NDs initially show a secondary peak eluting at approximately 12 min. This peak has a Mw of approximately 400 kDa and was observed to slowly decrease in intensity after incubation at moderate temperatures, whereas the main ND peak simultaneously increased, suggesting inter-particle exchange of components. Even at relatively mild temperatures, NDs containing unsaturated lipids

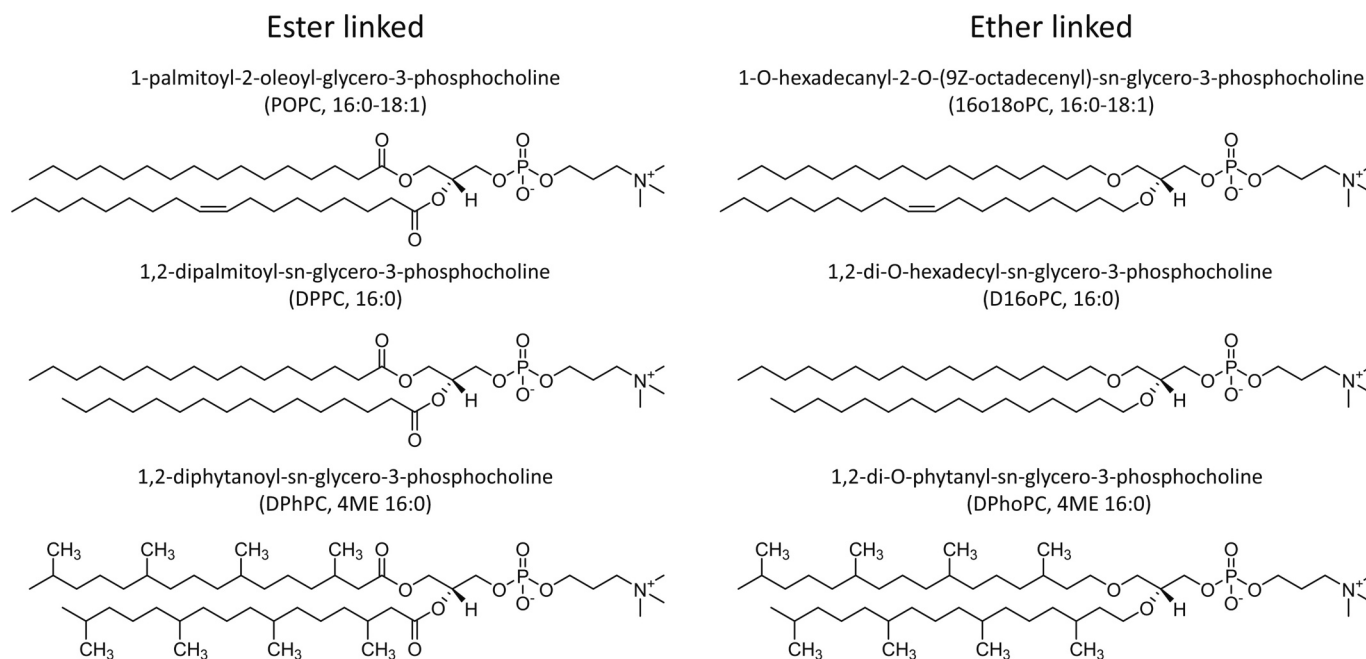


Fig. 1. Chemical structures of the phospholipids used for ND assembly.

Table 1

Size and composition of NDs assembled with different PC lipids measured by SEC-MALS and analyzed using the protein conjugate method. Molecular weights and composition determined by SEC-MALS are averages of six replicate measurements, DLS averaged R_h and % PD data are averages of six replicate measurements \pm two standard deviations of the mean.

	POPC 16:0-18:1	16o18oPC 16:0-18:1	DPPC 16:0	D16oPC 16:0	DPhPC 4ME 16:0	DPhoPC 4ME 16:0
Mw ND (kDa)	147 \pm 4	157 \pm 5	181 \pm 3	180 \pm 9	144 \pm 3	145 \pm 5
Mw protein (kDa)	49 \pm 4	53 \pm 4	49 \pm 2	48 \pm 5	75 \pm 4	77 \pm 6
Mw lipid (kDa)	98 \pm 1	105 \pm 2	133 \pm 2	133 \pm 4	69 \pm 1	68 \pm 2
Copies of MSP1D1	2.0 \pm 0.1	2.1 \pm 0.2	2.0 \pm 0.1	1.9 \pm 0.2	3.0 \pm 0.2	3.1 \pm 0.2
Lipids / MSP1D1	64.5 \pm 0.9	71 \pm 1	92 \pm 4	97 \pm 9	27 \pm 2	27 \pm 3
DLS hydrodynamic radius (R_h) (nm)	4.9 \pm 0.2	5.0 \pm 0.1	5.2 \pm 0.1	5.0 \pm 0.2	5.1 \pm 0.1	5.1 \pm 0.1
DLS % polydispersity	12 \pm 7	7 \pm 2	12 \pm 8	12 \pm 6	11 \pm 6	12 \pm 5

aggregated profoundly in a matter of hours. Especially 16o18oPC, the ether-linked analog of POPC forms unstable NDs. Within the first 5 h of incubation at 37 °C, ~47 % and ~12 % of the 16o18oPC - and POPC NDs had aggregated, respectively. The saturated lipid NDs are much more stable, showing <10 % loss after 24 h of incubation at 37 °C. Another interesting observation from the elution profiles in Fig. 4 is that for NDs assembled with linear chain fatty acids, the main ND peak is shifting to the right after incubation at 50 °C. This indicates that the hydrodynamic radius (R_h) of the NDs is decreasing over time. Compositional analysis by SEC-MALS shows that the NDs still contain the same number of MSP1D1 molecules, so the shrinkage must be attributed to loss of lipid. DPPC- and D16oPC NDs lose as much as ~23 % of the initial lipid cargo after 24 h of incubation at 50 °C. Interestingly, the phytanyl lipid NDs were very stable at 37 °C, and do not shrink, even after prolonged incubation at 50 °C.

3. Discussion and conclusions

Major challenges remain in the design and controlled delivery of stable (bio-)pharmaceuticals. Nanoparticles can enhance circulation lifetime, protect against chemical and enzymatic denaturation as well as boost the efficacy of a drug. Increasing demand for nanoparticle technologies has recently been emphasized by the corona virus pandemic and the consequent mass vaccination effort. In this work, NDs were prepared using various ether- and ester-linked linear and branched

lipids. Surprisingly, phytanyl lipid NDs are shown to contain three copies of the scaffold protein and not the canonical dimer. A triple scaffold configuration was reported before in the cryo-EM structure of a rotary vacuolar adenosine triphosphatase inside NDs [42]. The need for a third scaffold molecule was ascribed to the large hydrophobic surface of the triphosphatase c-ring. In “empty” NDs it seems unlikely that a phytanyl bilayer can accommodate a stack of three MSPs, because molecular dynamics (MD) simulations showed that DPhPC bilayers have comparable head-to-head thickness as linear chain lipid POPC bilayers [40]. For spherical HDL, a “trefoil”-like conformation has been described. The trefoil model has three ApoA1 belts bent at 120° angles, effectively maintaining the same intermolecular contacts as in the double belt [43,44]. Cross-linking–mass spectrometry has shown that these contacts remain constant when going from the discoidal form to spherical “multifoil” HDL particles, comprising three or more copies of ApoA1 [43,45]. A trefoil conformation would impose curvature on the membrane, which could be accounted for by bending of the phytanyl lipid tails, as described for DPhPC based on MD simulations [46]. However, the number of phytanyl lipids per ND that follows from the experiments makes a trefoil conformation less likely. The inner diameter of a discoidal MSP1D1 ND is ~76 Å [18], from which a membrane surface area of *circa* 4500 Å² for each side of the ND can be calculated. Dividing by the area per lipid of 80.8 Å² which was determined for DPhPC by MD simulations [41], we initially estimated that a ND could contain approximately 110 phytanyl lipids over the two layers. The

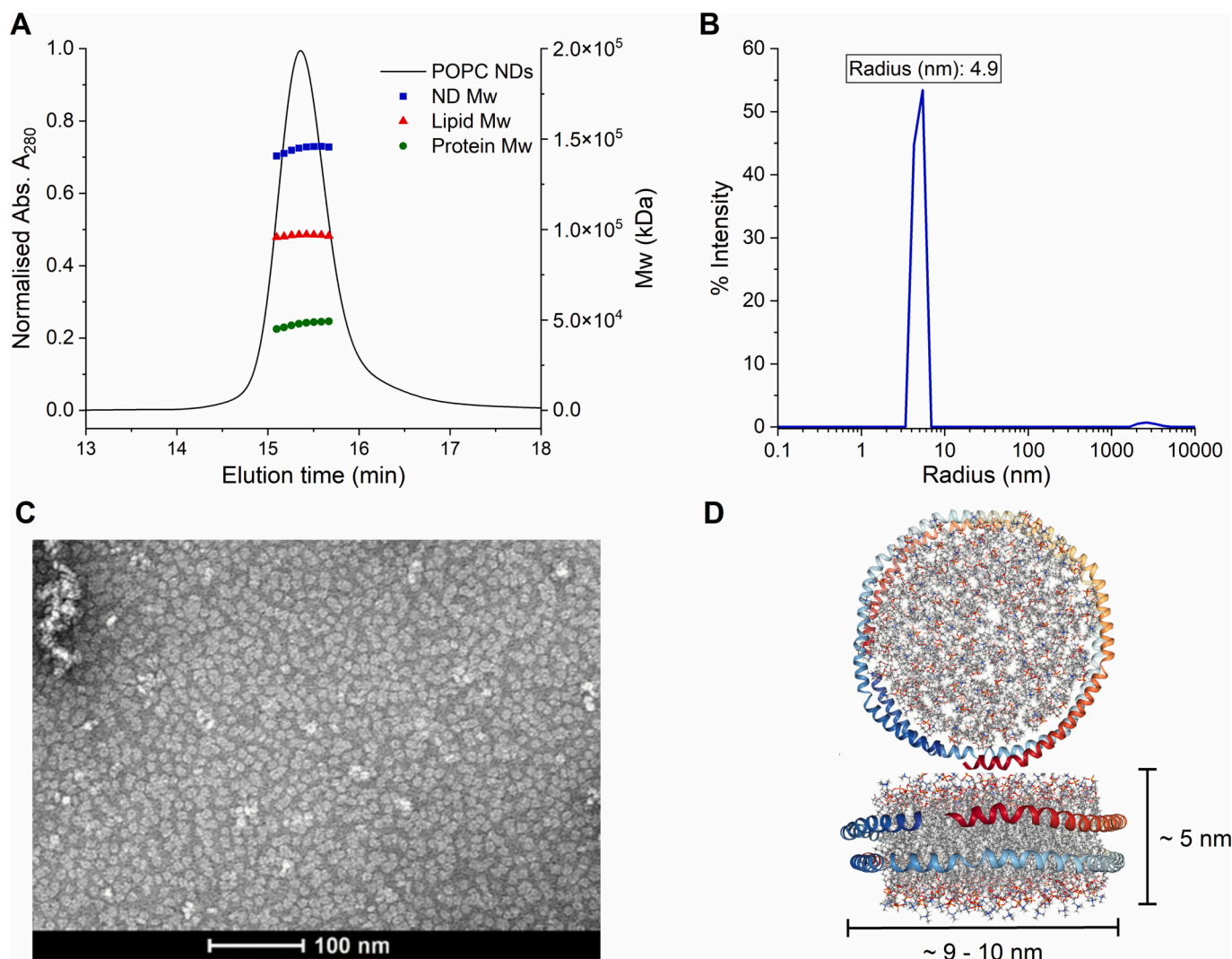


Fig. 2. Biophysical characterization of POPC NDs. (A) NDs were analyzed using SEC-MALS. The total ND, protein and lipid molecular weight (fractions) were determined by protein conjugate analysis. (B) Dynamic light scattering of POPC NDs shows a monodisperse ND size of ~ 4.8 nm radius. (C) Similarly, negative stain TEM shows a homogeneous distribution of NDs. (D) A schematic representation of NDs comprised of two MSP1D1 proteins and 126 POPC lipids was generated using the NDs builder in CHARMM GUI and is shown for illustrative purposes [60].

experimental number is significantly lower, about 80–90 lipids per NDs. For a trefoil conformation, the maximum lipid capacity would be approximately 1.5 times higher than for a flat ND, so there would be a large lipid deficit. Thus, how a relatively small phytanyl membrane can accommodate three MSP molecules remains unclear and warrants further, structural research.

By systemically comparing the stability of NDs composed of different lipids we are able to provide guidelines for the production of thermostable NDs, which are likely broadly applicable to LNP development. In line with previous research, NDs prepared with lipids that contain two saturated fatty acids ($2 \times 16:0$) are much more thermostable than ones with lipids that contain one unsaturated fatty acid (16:0, 18:1). No significant difference in ND thermostability was found between saturated ether and ester lipids. In contrast, NDs prepared with one unsaturated (18:1) and one saturated (16:0) ether-linked fatty acid (16o18oPC) are less stable than NDs containing the equivalent ester-linked fatty acids (POPC). Outer membranes of all thermophilic archaea and some thermophilic bacteria possess ether lipids, though almost always with saturated fatty acids [47]. For a long time it was debated whether ether linkages, as well as branching and complex cyclopentane-containing tetraether lipids found in thermophiles, are evolutionary adaptations required for survival at the extreme [48–53].

However, not all organisms possessing the associated “thermostable lipids” found in thermophiles are actually thermophilic. Phytanyl lipids, for instance, are present in a liquid crystalline state over the entire biological temperature range and have been identified in extremophiles and mesophiles alike. Thus, such ether-linked phytanyl lipids are perhaps more aptly described as “heat tolerant” lipids [47]. The fact that branched lipids provide a stable and functional bilayer over a wide temperature range is very attractive for the reconstitution of membrane proteins and LNP development. Lipids with linear, saturated fatty acids (DPPC and D16oPC) on the contrary, have a relatively high T_m and thus are present in the gel phase at moderate temperature, which can impair membrane protein function. The ideal lipid reconstitution composition depends greatly on the target protein. This is especially true for membrane proteins whose functions may be substantially influenced by membrane fluidity and curvature or is even directly regulated by lipid cofactors [54]. The physicochemical interaction at the membrane may be less important for example when a “passive” viral membrane protein is incorporated, where the sole function is to elicit an effective immune response against a particular antigen. In such cases the lipid composition can be optimized for factors like thermostability and immunogenicity.

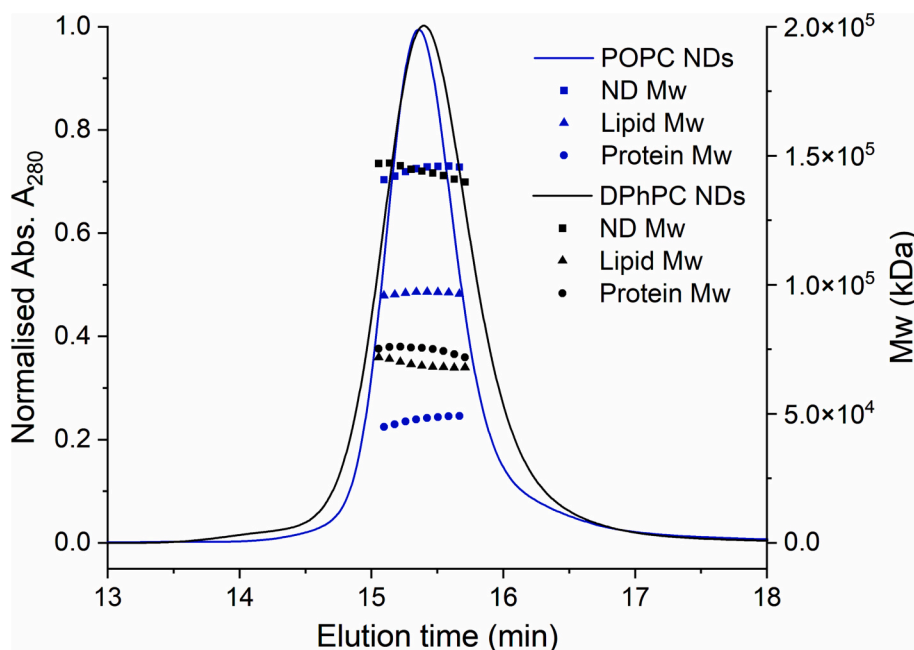


Fig. 3. DPhPC NDs have a protein-to-lipid ratio that is much higher than found in the canonical double MSP1D1 ND of POPC lipids. However, both types of NDs have similar hydrodynamic volumes and ND Mw.

4. Materials & methods

4.1. Lipid handling and concentration determination

Chemically synthesized 16o18oPC lipids were bought from Merca-chem BV. All other synthetic lipids were bought from Avanti polar lipids. Lipid aliquots were stored at -20°C as powder or chloroform/methanol aliquots. Lipids were taken directly from powder stocks into a pre-weighed glass vials with teflon-lined caps. Lipid in chloroform/methanol stocks were pipetted using Hamilton syringes into pre-weighed glass vials and dried under a gentle stream of nitrogen gas and kept overnight inside a vacuum chamber at <0.1 mPa. Lipid powder or films were weighed on a Sartorius Cubis® MCA6.6S-2S00-M microbalance. This procedure was compared to total phosphorous concentration determination of the lipid stock solutions and produced comparable and reproducible measures of the total lipid amounts [55].

4.2. Nanodisc assembly procedures

The MSP1D1 gene was synthesized by GeneArt (Thermo Fisher Scientific) and cloned into the pET28a vector using *NcoI* and *BamHI* restriction enzymes. MSP1D1 was expressed in BL21(DE3) pLysS *E. coli* cells in terrific broth (TB) media in baffled shake flasks at 37°C , 200 rpm. Gene expression was induced with 1 mM IPTG at $\text{OD}_{600} = 2\text{--}2.5$ and cells were harvested 5 h after induction. MSP1D1 was purified by nickel affinity chromatography as described previously [2]. Dried lipids were solubilized by addition of 100 mM sodium cholate stock solution. The samples were heated under warm tap water, vortexed and sonicated intermittently for approximately 30–45 min until the solution became completely transparent. MSP1D1 was added at the appropriate molar ratio determined for each of the lipids (Table 2). The ND stoichiometric protein-to-lipid ratios were estimated by calculating the composition of a maximally filled ND by dividing the ND membrane surface area by the area per lipid used. NDs were produced at three different stoichiometric ratios close to the estimation. After initial SEC purification, aggregated fractions, NDs and lipid poor fractions were identified by comparing to a gel filtration standard (Bio-Rad #1511901). The resulting lipid and protein composition of each fraction were analyzed in detail by SEC-MALS and the lipid: MSP1D1 ratio of the maximally filled ND was

used for subsequent assembly experiments.

The reconstitution mixtures were prepared at a final concentration of 5 mM lipid and 20 mM cholate and left to equilibrate near the main phase transition temperature of the lipids used for 45 min. Phytanyl lipid NDs were equilibrated and assembled at 4°C . The detergent was removed by 48 h dialysis at the respective equilibration temperatures in a 10 kDa MWCO slide-a-lyzer MINI dialysis tube (Thermo Fisher) containing 5 g amberlite bio-beads XAD-2 on the opposing side of the dialysis membrane. It was observed during previous experiments that direct contact with biobeads resulted in significant loss of MSP1D1 and reduced ND yields by up to 50 %. MSP1D1 and NDs concentration were determined by absorbance spectroscopy and quantification of the peak at A_{280} using a theoretical extinction coefficient of $\epsilon_{280} = 21,430 \text{ M}^{-1}\cdot\text{cm}^{-1}$ for MSP1D1.

4.3. SEC-MALS protein conjugate analysis of NDs

The absolute ND Mw was measured using a SEC-MALS system comprising a miniDAWN® TREOS®, DynaPro® NanoStar® DLS, Opti-lab differential refractometer (Wyatt technology) and 1260 Infinity II multiple wavelength absorbance detector (Agilent). The composition of NDs and aggregates after heat treatment were determined using the protein conjugate method present in the ASTRA 8 software package. After selecting the peak area of interest and defining the $\text{dn}/\text{dc}_{\text{protein}}$, $\text{dn}/\text{dc}_{\text{lipid}}$, $\epsilon_{280, \text{protein}}$ and $\epsilon_{280, \text{lipid}}$, the software reports the Mw of the complex, the protein fraction and the “modifier” (lipid fraction) at each data slice throughout the peak selection. The program SEDFIT was used to calculate a theoretical $\text{dn}/\text{dc}_{\text{protein}}$ of 1.88 mL/g and weight averaged extinction coefficient of $0.869 \text{ mg/mL}^{-1}\cdot\text{cm}^{-1}$ for MSP1D1 based on its amino acid sequence [59]. A theoretical $\text{dn}/\text{dc}_{\text{lipid}}$ of 0.16 mL/g was used for all lipids. The ND stoichiometric protein-to-lipid ratios were determined by dividing the resulting protein and lipid molecular weight fractions by their respective molecular weights and calculating the ratio between the ND components.

4.4. NDs thermostability comparison by analytical SEC

NDs were purified by SEC on a Superdex 200–10/300 GL column. All samples were normalized for concentration by A_{280} signal and divided

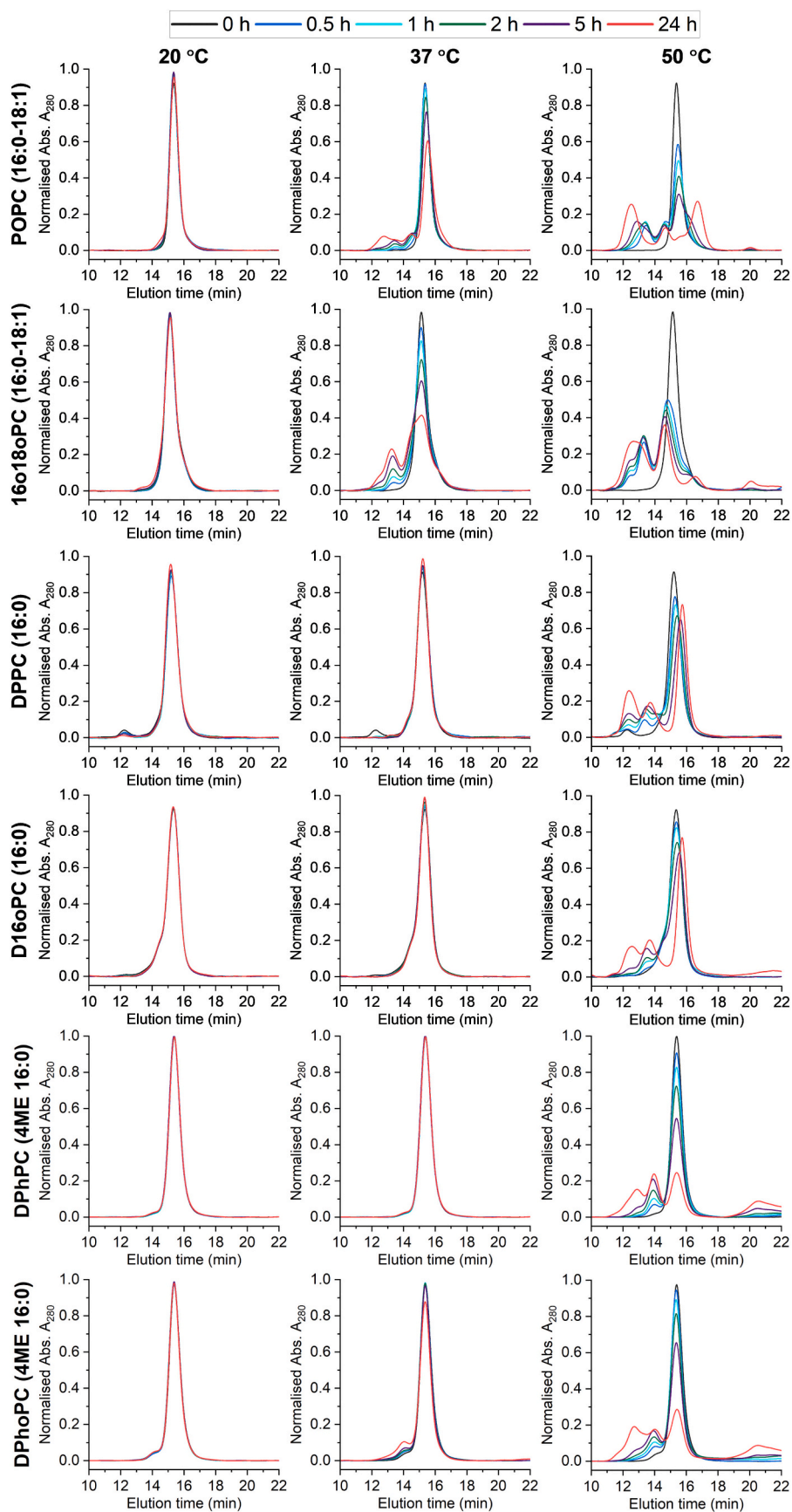


Fig. 4. NDs were analyzed by SEC after incubation at 20°C, 37°C or 50°C. Each panel shows the elution profiles (A_{280}) of NDs after incubation for different times at the respective temperatures. Every second row shows results for the NDs with the ether equivalent of the ester lipids in the row above.

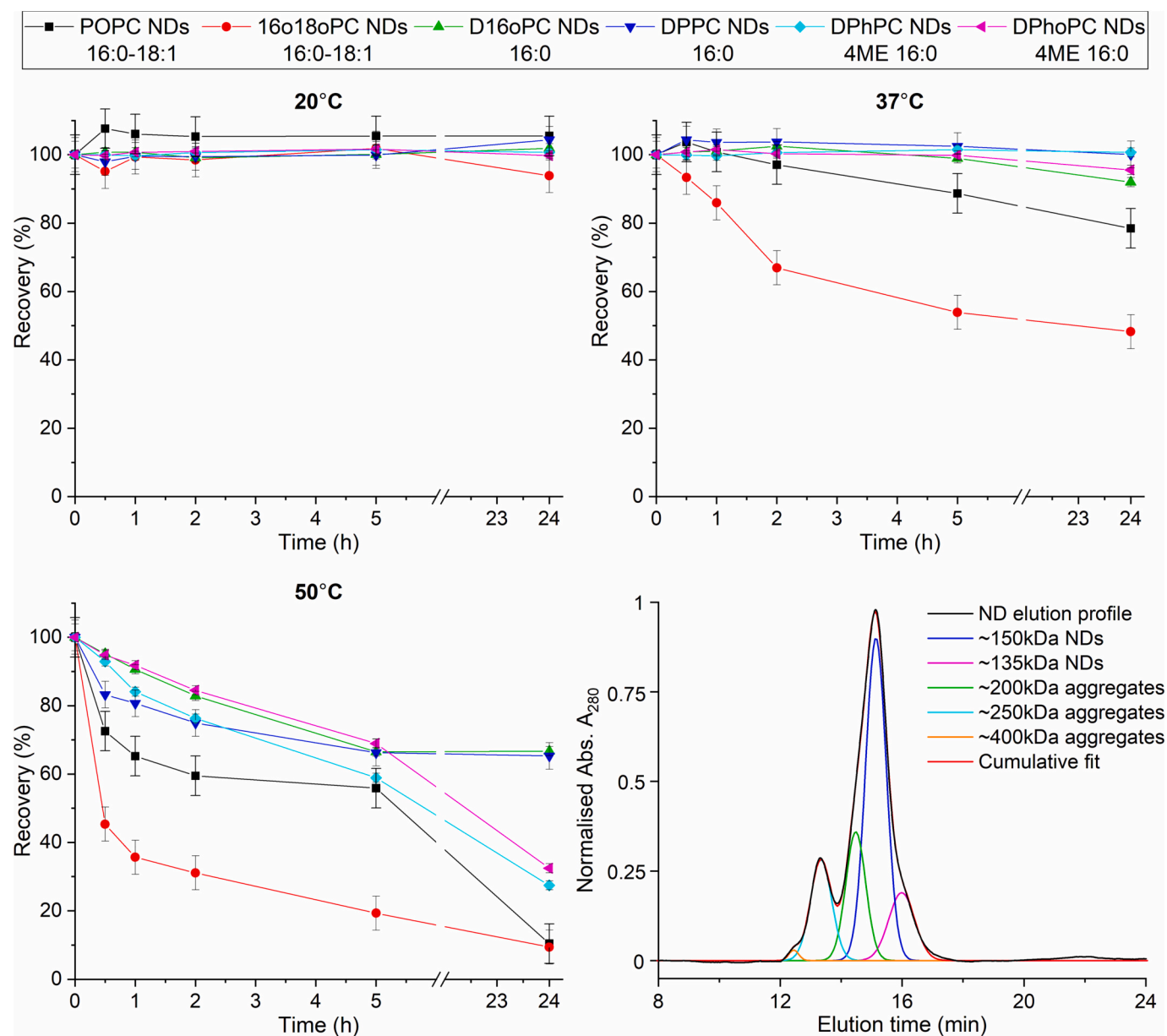


Fig. 5. Percent recovery of NDs prepared with different lipids is shown against incubation time at 20 °C, 37 °C and 50 °C. The ND elution profiles (A_{280}) from Fig. 4 were deconvoluted into separate peaks as shown in the bottom right panel. The fitted ND peak areas were compared against the peak areas measured for the control samples kept at 4 °C. In the example two different sized ND populations were found, of 135 kDa and 150 kDa, so the combined surface area was used to calculate the ND recovery. Error bars indicate two standard deviations of mean surface area measured under stable conditions.

into separate replicate tubes. NDs were heated at 20 °C, 37 °C and 50 °C in a thermocycler with lid heating enabled at the same temperatures to reduce evaporation or kept at 4 °C as negative control. After heat treatment, NDs were rapidly chilled on ice, centrifuged briefly and transferred to an Agilent autosampler for injection on SEC. Identical volumes of heat exposed NDs were injected on a Superdex 200 10/300 GL for each sample. The relative ND recovery was determined by deconvolution of the absorbance peaks (A_{280}) using the fit peaks pro application in OriginPro 2022® (OriginLab). Here, the peak mean and maxima were manually estimated followed by a nonlinear least square fitting of a sum of Gaussian distributions. The ND fit peak surface area was determined for each of the samples after heating.

4.5. Dynamic light scattering

DLS R_h values were measured at a concentration of 4–12 μ M NDs

using disposable cuvettes inside a DynaPro® Nanostar® DLS (Wyatt technology), in a buffer containing 100 mM NaPi, pH 7.4 and 100 mM NaCl. Samples were centrifuged for 5 min at 13 k rpm in a micro-centrifuge and left to equilibrate in the DLS instrument to 20 °C for 3 min after which 10 acquisitions of 5 s were performed per measurement. Data acquisition and analysis was done using Dynamics™ software (Wyatt technology). Since both cumulants and regularization algorithms closely fitted the auto correlation data, it was decided to report the average R_h and two times standard deviations derived from the cumulants fit for each type of ND from 10 repeat measurements. The % intensity distribution which is derived directly from the autocorrelation function gives the most accurate distribution of R_h and were thus reported.

Table 2

Optimal reconstitution conditions determined for NDs assembled with different lipids.

Lipid abbreviation	ND assembly ratio (Lipid/MSP1D1)	ND assembly temp. (°C)	Lipid theoretical mass (Da)	Lipid main phase transition temp. T _m (°C)
POPC (16:0–18:1)	65	4	760	-2 [56]
16o18oPC (16:0–18:1)	75	4	732	Not determined
DPPC (16:0)	90	40	734	41.6 [57]
D16oPC (16:0)	90	40	706	43.6 [57]
DPhPC (4ME 16:0)	30	4	846	None (-120 to 120) [58]
DPhoPC (4ME 16:0)	30	4	818	None (-120 to 120)

4.6. Negative stain transmission electron microscopy

Three microliters of ND solution at a concentration of 1 μM was pipetted onto a freshly glow-discharged TEM grid (Cu, 200 Mesh) with a continuous carbon support film and incubated for 1 min. Afterwards, the sample was wicked away with filter paper and stained with a 2 % uranyl formate solution for 30 s. Micrographs were collected on a Tecnai T12 BioTWIN operating at 120 kV.

Declaration of competing interest

The authors declare the following financial interests/potential relationships which may be considered as potential competing interests:

Marcellus Ubbink reports financial support was provided by The Dutch Research Council (NWO). Marcellus Ubbink reports a relationship with Batavia Biosciences BV that includes: funding grants. Marcellus Ubbink reports a relationship with ZoBio BV that includes: funding grants. The authors disclose a potential competing interest due to an ongoing patent filing related to the topics discussed in this study. The project was funded by the Dutch Research Council with financial contributions by Batavia Biosciences B.V. and ZoBio B.V.

Acknowledgements

The Dutch Research Council (NWO) is acknowledged for financial support of the project through the Applied and Engineering Sciences (AES), grant 16259 to MU. Dr. Abhinav Luthra and Dr. Maithili Krishnan-Schmieden are gratefully acknowledged for their advice on ND preparations. Dr. Maithili Krishnan-Schmieden is also acknowledged for the modeling of NDs using CHARMM GUI. Dr. Thomas H. Sharp and Dr. Willem Noteborn are acknowledged for the imaging of NDs using negative stain transmission electron microscopy.

Appendix A. Supplementary data

Supplementary data to this article can be found online at <https://doi.org/10.1016/j.bbmem.2023.184239>.

References

- T.H. Bayburt, J.W. Carlson, S.G. Sligar, Reconstitution and imaging of a membrane protein in a nanometer-size phospholipid bilayer, *J. Struct. Biol.* 123 (1998) 37–44, <https://doi.org/10.1006/jsbi.1998.4007>.
- T.H. Bayburt, Y.V. Grinkova, S.G. Sligar, Self-assembly of discoidal phospholipid bilayer nanoparticles with membrane scaffold proteins, *Nano Lett.* 2 (2002) 853–856.
- O. Gursky, Structural stability and functional remodeling of high-density lipoproteins, *FEBS Lett.* 589 (2015) 2627–2639, <https://doi.org/10.1016/j.febslet.2015.02.028>.
- J.B. Simonsen, Evaluation of reconstituted high-density lipoprotein (rHDL) as a drug delivery platform - a detailed survey of rHDL particles ranging from biophysical properties to clinical implications, *Nanomedicine Nanotechnology Biol. Med.* 12 (2016) 2161–2179, <https://doi.org/10.1016/j.nano.2016.05.009>.
- D. Pedersen, J.B. Simonsen, A systematic review of the biodistribution of biomimetic high-density lipoproteins in mice, *J. Control. Release* 328 (2020) 792–804, <https://doi.org/10.1016/j.jconrel.2020.09.038>.
- W.J.M. Mulder, M.M.T. Van Leent, M. Lameijer, E.A. Fisher, Z.A. Fayad, C. Pérez-Medina, High-density lipoprotein Nanobiologics for precision medicine, *Acc. Chem. Res.* 51 (2018) 127–137, <https://doi.org/10.1021/acs.accounts.7b00339>.
- C. Feng, Y. Li, B.E. Ferdows, D.N. Patel, J. Ouyang, Z. Tang, N. Kong, E. Chen, W. Tao, Emerging vaccine nanotechnology: from defense against infection to sniping cancer, *Acta Pharm. Sin. B* 12 (2022) 2206–2223, <https://doi.org/10.1016/j.apsb.2021.12.021>.
- C.M. Gibson, S. Korjian, P. Tricoci, Y. Daaboul, M. Yee, P. Jain, J.H. Alexander, P. G. Steg, A.M. Lincoff, J.J.P. Kastelein, R. Mehran, D.M. D'Andrea, L.I. Deckelbaum, B. Merkely, M. Zarebinski, T.O. Ophuis, R.A. Harrington, Safety and tolerability of CSL112, a reconstituted, infusible, plasma-derived apolipoprotein A-I, after acute myocardial infarction: the AEGIS-I trial (ApoA-I event reducing in ischemic syndromes I), *Circulation.* 134 (2016) 1918–1930, <https://doi.org/10.1161/CIRCULATIONAHA.116.025687>.
- C.M. Gibson, J.J.P. Kastelein, A.T. Phillips, P.E. Aylward, M.K. Yee, M. Tendera, S. J. Nicholls, S. Pocock, S.G. Goodman, J.H. Alexander, A.M. Lincoff, C. Bode, D. Duffy, M. Heise, G. Berman, S.J. Mears, P. Tricoci, L.I. Deckelbaum, P.G. Steg, P. Ridker, R. Mehran, Rationale and design of ApoA-I event reducing in ischemic syndromes II (AEGIS-II): a phase 3, multicenter, double-blind, randomized, placebo-controlled, parallel-group study to investigate the efficacy and safety of CSL112 in subjects after acute myocardial infarction, *Am. Heart J.* 231 (2021) 121–127, <https://doi.org/10.1016/j.ahj.2020.10.052>.
- R. Kuai, W. Yuan, S. Son, J. Nam, Y. Xu, Y. Fan, A. Schwendeman, J.J. Moon, Elimination of established tumors with nanodisc-based combination chemioimmunotherapy, *Sci. Adv.* 4 (2018) 1–14, <https://doi.org/10.1126/sciadv.aao1736>.
- L. Scheetz, P. Kadiyala, X. Sun, S. Son, A.H. Najafabadi, M. Aikins, P.R. Lowenstein, A. Schwendeman, M.G. Castro, J.J. Moon, Synthetic high-density lipoprotein nanodiscs for personalized immunotherapy against gliomas, *Clin. Cancer Res.* 26 (2020) 4369–4380, <https://doi.org/10.1158/1078-0432.CCR-20-0341>.
- A.H. Najafabadi, Z.I.N. Abadi, M.E. Aikins, K.E. Foulds, M.M. Donaldson, W. Yuan, E.B. Okeke, J. Nam, Y. Xu, P. Weerappuli, T. Hetrick, D. Adams, P.A. Lester, A. M. Salazar, D.H. Barouch, A. Schwendeman, R.A. Seder, J.J. Moon, Vaccine nanodiscs plus polyI:CLC elicit robust CD8+ T cell responses in mice and non-human primates, *J. Control. Release* 337 (2021) 168–178, <https://doi.org/10.1016/j.jconrel.2021.07.026>.
- M.M.J. Cox, J.R. Hollister, FluBlok, a next generation influenza vaccine manufactured in insect cells, *Biologicals.* 37 (2009) 182–189, <https://doi.org/10.1016/j.biologicals.2009.02.014>.
- J. Pollet, W. Chen, U. Strych, Recombinant Protein Vaccines, a Proven Approach against Coronavirus Pandemics, 2020.
- T.H. Tulchinsky, Maurice Hilleman, Creator of vaccines that changed the world, *Case Stud. Public Heal.* (2018) 443–470, <https://doi.org/10.1016/b978-0-12-804571-8.00003-2>.
- H. Malik, F.H. Khan, H. Ahsan, Human papillomavirus: current status and issues of vaccination, *Arch. Virol.* 159 (2014) 199–205, <https://doi.org/10.1007/s00705-013-1827-z>.
- P. Bhattacharya, S. Grimme, B. Ganesh, A. Gopisetty, J.R. Sheng, O. Martinez, S. Jayarama, M. Artinger, M. Meriggioli, B.S. Prabhakar, Nanodisc-incorporated hemagglutinin provides protective immunity against influenza virus infection, *J. Virol.* 84 (2010) 361–371, <https://doi.org/10.1128/jvi.01355-09>.
- I.G. Denisov, M.A. McLean, A.W. Shaw, Y.V. Grinkova, S.G. Sligar, Thermotropic phase transition in soluble nanoscale lipid bilayers, *J. Phys. Chem. B* 109 (2005) 15580–15588, <https://doi.org/10.1021/jp051385g>.
- D.M. Kehlenbeck, I. Josts, J. Nitsche, S. Busch, T. Forsyth, H. Tidow, Comparison of lipidic carrier systems for integral membrane proteins - MsbA as case study, *Biol. Chem.* 400 (2019) 1509–1518, <https://doi.org/10.1515/hsz-2019-0171>.
- M.L. Nasr, G. Wagner, Covalently circularized nanodiscs; challenges and applications, *Curr. Opin. Struct. Biol.* 51 (2018) 129–134, <https://doi.org/10.1016/j.sbi.2018.03.014>.
- M.L. Nasr, D. Baptista, M. Strauss, Z.Y.J. Sun, S. Grigoriu, S. Huser, A. Plückthun, F. Hagn, T. Walz, J.M. Hogle, G. Wagner, Covalently circularized nanodiscs for studying membrane proteins and viral entry, *Nat. Methods* 14 (2016) 49–52, <https://doi.org/10.1038/nmeth.4079>.
- S. Zhang, Q. Ren, S.J. Novick, T.S. Strutzenberg, P.R. Griffin, H. Bao, One-step construction of circularized nanodiscs using SpyCatcher-SpyTag, *Nat. Commun.* 12 (2021) 1–9, <https://doi.org/10.1038/s41467-021-25737-7>.
- Q. Ren, S. Zhang, H. Bao, Circularized fluorescent nanodiscs for probing protein–lipid interactions, *Commun. Biol.* 5 (2022) 1–7, <https://doi.org/10.1038/s42003-022-03443-4>.
- M. Wadsäter, S. Maric, J.B. Simonsen, K. Mortensen, M. Cardenas, The effect of using binary mixtures of zwitterionic and charged lipids on nanodisc formation and stability, *Soft Matter* 9 (2013) 2329–2337, <https://doi.org/10.1039/c2sm27000e>.
- N.T. Johansen, F.G. Tidemand, T.T.T.N. Nguyen, K.D. Rand, M.C. Pedersen, L. Arleth, Circularized and solubility-enhanced MSPs facilitate simple and high-yield production of stable nanodiscs for studies of membrane proteins in solution, *FEBS J.* 286 (2019) 1734–1751, <https://doi.org/10.1111/febs.14766>.
- M. Guha, D.L. Gantz, O. Gursky, Effects of acyl chain length, unsaturation, and pH on thermal stability of model discoidal HDLs, *J. Lipid Res.* 49 (2008) 1752–1761, <https://doi.org/10.1194/jlr.M800106-JLR200>.

- [27] H.J. Pownall, Q. Pao, J.B. Massey, Acyl chain and headgroup specificity of human plasma lecithin:cholesterol acyltransferase. Separation of matrix and molecular specificities, *J. Biol. Chem.* 260 (1985) 2146–2152, [https://doi.org/10.1016/s0021-9258\(18\)89529-1](https://doi.org/10.1016/s0021-9258(18)89529-1).
- [28] A.K. Soutar, C.W. Garner, H.N. Baker, J.T. Sparrow, R.L. Jackson, A.M. Gotto, L. C. Smith, Effect of the human plasma apolipoproteins and phosphatidylcholine acyl donor on the activity of lecithin: cholesterol acyltransferase, *Biochemistry*. 14 (1975) 3057–3064, <https://doi.org/10.1021/bi00685a003>.
- [29] W.S. Davidson, K.L. Gillotte, S. Lund-Katz, W.J. Johnson, G.H. Rothblat, M. C. Phillips, The effect of high density lipoprotein phospholipid acyl chain composition on the efflux of cellular free cholesterol, *J. Biol. Chem.* 270 (1995) 5882–5890, <https://doi.org/10.1074/jbc.270.11.5882>.
- [30] M.V. Fawaz, S.Y. Kim, D. Li, R. Ming, Z. Xia, K. Olsen, I.D. Pogozheva, J.J. G. Tesmer, A. Schwendeman, Phospholipid component defines pharmacokinetic and pharmacodynamic properties of synthetic high-density lipoproteins, *J. Pharmacol. Exp. Ther.* 372 (2020) 193–204, <https://doi.org/10.1124/JPET.119.257568>.
- [31] S.F. Gilmore, T.S. Carpenter, H.I. Ingólfsson, S.K.G. Peters, P.T. Henderson, C. D. Blanchette, N.O. Fischer, Lipid composition dictates serum stability of reconstituted high-density lipoproteins: implications for: in vivo applications, *Nanoscale*. 10 (2018) 7420–7430, <https://doi.org/10.1039/c7nr09690a>.
- [32] G.B. Patel, G.D. Sprott, Archaeobacterial ether lipid liposomes (archaeosomes) as novel vaccine and drug delivery systems, *Crit. Rev. Biotechnol.* 19 (1999) 317–357, <https://doi.org/10.1080/0738-859991229170>.
- [33] K. Haq, Y. Jia, L. Krishnan, Archaeal lipid vaccine adjuvants for induction of cell-mediated immunity, *Expert Rev. Vaccines* 15 (2016) 1557–1566, <https://doi.org/10.1080/14760584.2016.1195265>.
- [34] N. Adamiak, K.T. Krawczyk, C. Loch, M. Kowalewicz-Kulbat, Archaeosomes and gas vesicles as tools for vaccine development, *Front. Immunol.* 12 (2021) 1–11, <https://doi.org/10.3389/fimmu.2021.746235>.
- [35] B. Akache, F.C. Stark, Y. Jia, L. Deschatelets, R. Dudani, B.A. Harrison, G. Agbayani, D. Williams, M.P. Jamshidi, L. Krishnan, M.J. McCluskie, Sulfated archaeol glycolipids: comparison with other immunological adjuvants in mice, *PLoS One* 13 (2018) 1–25, <https://doi.org/10.1371/journal.pone.0208067>.
- [36] B. Akache, T.M. Renner, A. Tran, L. Deschatelets, R. Dudani, B.A. Harrison, D. Duque, J. Haukenfrers, M.A. Rossotti, F. Gaudreault, U.D. Hemraz, E. Lam, S. Rognier, W. Chen, C. Gervais, M. Stuble, L. Krishnan, Y. Durocher, M. J. McCluskie, Immunogenic and efficacious SARS-CoV-2 vaccine based on resistin-trimerized spike antigen SmT1 and SLA archaeosome adjuvant, *Sci. Rep.* 11 (2021) 21849, <https://doi.org/10.1038/s41598-021-01363-7>.
- [37] N.O. Fischer, A. Rasley, M. Corzett, M.H. Hwang, P.D. Hoepflich, C.D. Blanchette, Colocalized delivery of adjuvant and antigen using nanolipoprotein particles enhances the immune response to recombinant antigens, *J. Am. Chem. Soc.* 135 (2013) 2044–2047, <https://doi.org/10.1021/ja3063293>.
- [38] R. Kuai, L.J. Ochyl, K.S. Bahjat, A. Schwendeman, J.J. Moon, Designer vaccine nanodiscs for personalized cancer immunotherapy, *Nat. Mater.* 16 (2017) 489–498, <https://doi.org/10.1038/NMAT4822>.
- [39] D. Foster, M.J. Havinga, Thermally Stable Vaccines Based on Ether Lipids and Native Viral Envelope Proteins. WO 2016/187118 Al. WIPO |PCT, n.d. <https://patents.google.com/patent/WO2016187118A1/en>.
- [40] S. Tristram-Nagle, D.J. Kim, N. Akhuzada, N. Kuerka, J.C. Mathai, J. Katsaras, M. Zeidel, J.F. Nagle, Structure and water permeability of fully hydrated diphytanoylPC, *Chem. Phys. Lipids* 163 (2010) 630–637, <https://doi.org/10.1016/j.chemphyslip.2010.04.011>.
- [41] A. Rasouli, Y. Jamali, E. Tajkhorshid, O. Bavi, H.N. Pishkenari, Mechanical properties of ester- and ether-DPhPC bilayers: a molecular dynamics study, *J. Mech. Behav. Biomed. Mater.* 117 (2021), 104386, <https://doi.org/10.1016/j.jmbmm.2021.104386>.
- [42] S.H. Roh, M. Shekhar, G. Pintilie, C. Chipot, S. Wilkens, A. Singharoy, W. Chiu, Cryo-EM and MD infer water-mediated proton transport and autoinhibition mechanisms of Vo complex, *Sci. Adv.* 6 (2020) 1–10, <https://doi.org/10.1126/sciadv.abb9605>.
- [43] R.A.G.D. Silva, R. Huang, J. Morris, J. Fang, E.O. Gracheva, G. Ren, A. Kontush, W. G. Jerome, K.A. Rye, W.S. Davidson, Structure of apolipoprotein A-I in spherical high density lipoproteins of different sizes, *Proc. Natl. Acad. Sci. U. S. A.* 105 (2008) 12176–12181, <https://doi.org/10.1073/pnas.0803626105>.
- [44] R. Huang, R.A.G.D. Silva, W.G. Jerome, A. Kontush, M.J. Chapman, L.K. Curtiss, T. J. Hodges, W.S. Davidson, Apolipoprotein A-I structural organization in high-density lipoproteins isolated from human plasma, *Nat. Struct. Mol. Biol.* 18 (2011) 416–423, <https://doi.org/10.1038/nsmb.2028>.
- [45] C.J. Malajczuk, N.S. Gandhi, R.L. Mancera, Structure and intermolecular interactions in spheroidal high-density lipoprotein subpopulations, *J. Struct. Biol.* X. 5 (2021), 100042, <https://doi.org/10.1016/j.yjsbx.2020.100042>.
- [46] W. Shinoda, M. Mikami, T. Baba, M. Hato, Molecular dynamics study of the lipid bilayers: effects of the chain branching on the structure and dynamics, *AIP Conf. Proc.* 708 (2004) 352–353, <https://doi.org/10.1063/1.1764171>.
- [47] Y. Koga, Thermal adaptation of the archaeal and bacterial lipid membranes, *Archaea*. 2012 (2012), <https://doi.org/10.1155/2012/789652>.
- [48] M. De Rosa, A. Gambacorta, The lipids of archaeobacteria, *Prog. LipM Res.* 27 (1988) 153–175.
- [49] N.P. Ulrih, D. Gmajner, P. Raspor, Structural and physicochemical properties of polar lipids from thermophilic archaea, *Appl. Microbiol. Biotechnol.* 84 (2009) 249–260, <https://doi.org/10.1007/s00253-009-2102-9>.
- [50] P.L.G. Chong, U. Ayesa, V. Prakash Daswani, E.C. Hur, On physical properties of tetraether lipid membranes: effects of cyclopentane rings, *Archaea*. 2012 (2012), <https://doi.org/10.1155/2012/138439>.
- [51] S.M. Jensen, V.L. Neesgaard, S.L.N. Skjoldbjerg, M. Brandl, C.S. Ejsing, A. H. Treusch, The effects of temperature and growth phase on the lipidomes of *Sulfolobus islandicus* and *Sulfolobus tokodaii*, *Life*. 5 (2015) 1539–1566, <https://doi.org/10.3390/life5031539>.
- [52] K. Rastädter, D.J. Wurm, O. Spadiut, J. Quehenberger, The cell membrane of *Sulfolobus* spp.—homeoviscous adaptation and biotechnological applications, *Int. J. Mol. Sci.* 21 (2020), <https://doi.org/10.3390/ijms21113935>.
- [53] M. Salvador-Castell, M. Golub, N. Erwin, B. Demé, N.J. Brooks, R. Winter, J. Peters, P.M. Oger, Characterisation of a synthetic Archaeal membrane reveals a possible new adaptation route to extreme conditions, *Commun. Biol.* 4 (2021) 1–13, <https://doi.org/10.1038/s42003-021-02178-y>.
- [54] C. Cecchetti, J. Strauss, C. Stohrer, C. Naylor, E. Pryor, J. Hobbs, S. Tanley, A. Goldman, B. Byrne, A novel high-throughput screen for identifying lipids that stabilise membrane proteins in detergent based solution, *PLoS One* 16 (2021) 1–20, <https://doi.org/10.1371/journal.pone.0254118>.
- [55] Avanti Polar Lipids, Determination of Total Phosphorus, 2022 <https://avantilipids.com/tech-support/analytical-procedures/determination-of-total-phosphorus>.
- [56] D.R. Silvius, Thermotropic Phase Transitions of Pure Lipids in Model Membranes and their Modifications by Membrane Proteins, New York John Wiley Sons, Inc, 1982.
- [57] H. Matsuki, H. Okuno, F. Sakano, M. Kusube, S. Kaneshina, Effect of deuterium oxide on the thermodynamic quantities associated with phase transitions of phosphatidylcholine bilayer membranes, *Biochim. Biophys. Acta Biomembr.* 1712 (2005) 92–100, <https://doi.org/10.1016/j.bbamem.2005.03.005>.
- [58] H. Lindsey, N.O. Petersen, S.I. Chan, Physicochemical characterization of 1,2-diphytanoyl-sn-glycero-3-phosphocholine in model membrane systems, *BBA-Biomembranes* 555 (1979) 147–167, [https://doi.org/10.1016/0005-2736\(79\)90079-8](https://doi.org/10.1016/0005-2736(79)90079-8).
- [59] H. Zhao, P.H. Brown, P. Schuck, On the distribution of protein refractive index increments, *Biophys. J.* 100 (2011) 2309–2317, <https://doi.org/10.1016/j.bpj.2011.03.004>.
- [60] S. Jo, T. Kim, V.G. Iyer, W. Im, CHARMM-GUI: a web-based graphical user interface for CHARMM, *J. Comput. Chem.* 29 (2008) 1859–1865, <https://doi.org/10.1002/jcc.20945>.